ELSEVIER

International Journal of Mass Spectrometry 198 (2000) 1–14

International Journal of Mass Spectrometry

Review

C_2 binding energy in C_{60}

C. Lifshitz

Department of Physical Chemistry and The Farkas Center for Light Induced Processes, The Hebrew University of Jerusalem, Jerusalem 91904, Israel

Received 20 December 1999; accepted 27 January 2000

Abstract

This article reviews, on the basis of mass spectrometric experiments, the current status concerning the C_2 binding energy or evaporation energy in C_{60}, $D(C_{58}–C_2) = \Delta E_{vap}(C_{60})$. Kinetic energy release distributions, time-resolved metastable fractions, breakdown curves, and thermionic emission rates all point to $\Delta E_{vap}(C_{60}^+) \geq 9.5$ eV and $\Delta E_{vap}(C_{60}) \geq 10$ eV. These results are in agreement with high-level *ab initio* density functional theory calculations and with expectations from the known heats of formation of C_{60}, C_{70}, and C_2. The C_2 evaporation is characterized by a very loose transition state with a pre-exponential factor close to the calculated upper limit. (Int J Mass Spectrom 198 (2000) 1–14) © 2000 Elsevier Science B.V.

Keywords: C_{60}; Fullerenes; Binding energy; Evaporation energy; Appearance energies; Kinetic shifts; Kinetic energy release distributions; Metastable fractions; Breakdown curves; Transition state; Activation entropy; Gspann parameter; DFT calculations; Thermionic emission; Radiative decay; RRKM; Finite heat bath theory

1. Introduction

The value of the C_2 binding energy in C_{60}, i.e. the dissociation energy, $D(C_{58}–C_2)$ [1], of

$$C_{60} \rightarrow C_{58} + C_2 \quad (1)$$

has been very difficult to determine until recently. It is conceivable that a nearly final answer has been reached in the years 1997–1999 through several experimental results [2–4], which converged on a high level density functional theory (DFT) computational result [5]. The reasons for the difficulty in determining the dissociation energy experimentally will be reviewed, as will be the methods used to circumvent these difficulties. The value currently acceptable on the basis of these more recent determinations [2–5] is $D(C_{58}–C_2) \geq 10$ eV. This result is consistent with expectations [6,7], based on the heats of formation of C_{60} (g), C_{70} (g), and C_2 (g), which are all quite accurately known. Kappes and co-workers [7] have calculated a very useful value—the average C_2 loss enthalpy for

$$C_{70} \rightarrow C_{60} + 5C_2 \quad (2)$$

The average value obtained [7], 8.1 eV, forms a lower bound on the C_2 binding energy of C_{60}, $D(C_{58}–C_2)$, since C_{62} as well as the other fullerenes bridging the

E-mail: chavalu@vms.huji.ac.il

PII S1387-3806(00)00192-5

gap between C_{60} and C_{70} are considerably less stable than C_{60}.

The major remaining discrepancies are between the high value of $D(C_{58}–C_2) \geq 10$ eV and the very low dissociation energies ($\leq$5.1 eV) deduced from thermal experiments carried out at high temperatures [8,9].

2. Theory

Theoretical studies of reaction (1) were carried out by using semiempirical modified neglect of diatomic differential overlap [10], the local spin density approximation with a plane-wave basis [11], Hartree-Fock (HF) [12], gradient-corrected exchange-correlation density functionals like BLYP with HF densities [12], and tight-binding methods [13,14]. These all yielded dissociation energies around 11–12 eV or higher, whereas most experimental studies gave considerably lower values. The title of the recent theoretical study by Boese and Scuseria [5] is: "C_2 fragmentation energy of C_{60} revisited: theory disagrees with most experiments." This most recent theoretical study involved DFT, but was not subject to limitations, as the earlier study [12] was, in the computational programs used to obtain fully optimized geometries and self-consistent Kohn-Sham calculations with different functionals. Both gradient corrected and hybrid functionals were used with fully optimized geometries. Furthermore, the first second-order perturbation theory (MP2) calculation was performed on this problem with a polarized Gaussian basis set (6-31G*). Thus, the calculations at the DFT and MP2 levels of theory considerably improved upon all previous theoretical calculations carried out on this problem. Nevertheless, the results obtained [5] support an electronic fragmentation energy, D_e, around 10–11 eV in agreement with some of the earlier theoretical results, but in excess of most experimental results available at the time, which placed the dissociation energy, D_0, (including zero point energy) around 7–8 eV.

The difference between the C_2 dissociation (evaporation) energy of the C_{60}^+ cation by means of

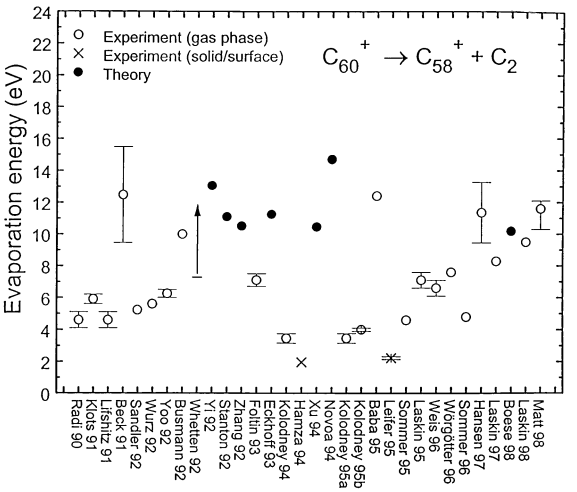

Fig. 1. Compilation of published dissociation energies for evaporation of C_2 from C_{60}^+ (adapted from [4]).

$$C_{60}^+ \rightarrow C_{58}^+ + C_2 \tag{3}$$

and that of neutral C_{60} is 0.54 eV,

$$D(C_{58}^+–C_2) = D(C_{58}–C_2) - 0.54 \text{ eV} \tag{4}$$

because the ionization energy of C_{60} is 0.54 eV higher than that of C_{58} [15,16]. Fig. 1 is a compilation of published evaporation energies of C_{60}^+ reproduced from [4]. It is clear that until 1997 most experiments gave results, namely $D(C_{58}^+–C_2) \leq 7$ eV, which were considerably lower than the theoretical results. The dissociation energy of C_{60} (and of C_{60}^+) may be one example showing the success of ab initio theory since it has been theory which insisted all along, in a consistent manner, that the binding energy was in excess of 10 eV.

3. Experiment

3.1. Introduction

We will concentrate here mainly on binding energy values derived through measurements on ionic systems. These include the following methods: (1) appearance energies (AEs); (2) kinetic energy release distributions (KERDs); (3) metastable fractions

(MFs); (4) electron impact induced fragmentation and breakdown curves; (5) the study of the competition between dissociation and thermionic emission. What are the experimental difficulties in determining the C_{60} dissociation energy using these methods? Some of the difficulties apply to most or all of the methods used and others are specific to certain methods and will be discussed in greater detail below. C_{60} is a molecule having 174 vibrational degrees of freedom in addition to having a very strong C_2 binding energy. As a result, the molecule is very "resilient" toward decomposition [17,18]. Furthermore, C_{60} is unique since when internally "hot" it undergoes cooling by emission in the visible—blackbody like radiative decay. This radiative energy loss is important under conditions similar to the ones that prevail in typical mass spectrometric devices [19,20]. The radiative cooling partially suppresses dissociation or "evaporative cooling" [21]. All of this causes the dissociation of C_{60}^+ to require large excess energies, a point that will be discussed in greater detail below.

Threshold photoelectron–photoion coincidence (TPEPICO) spectroscopy is one of the most precise methods for determining the heats of formation of ions [22]. The detection of internal energy selected ions means that the appearance energies for the formation of products upon the dissociative ionization of a neutral molecule can be determined accurately. Gaseous C_{60} could in principle be studied by TPEPICO by using synchrotron radiation as the light source, however, experiments applying this method failed to deliver a significant signal since no threshold electrons were observed for C_{60} photoionization [23]. There are thus no direct determinations of the absolute rate energy dependence, i.e. the dependence of the microcanonical rate constant, $k(E)$, for reaction (3) on energy has not been directly measured. By the same token, direct measurements of breakdown curves for the C_{60}^+ reaction system are not available either. Many of the indirect measurements require elaborate modeling that requires knowledge concerning the degree of tightness or looseness of the transition state for reaction (3). This has shown up in Rice-Ramsperger-Kassel-Marcus (RRKM) calculations of $k(E)$ as well as in the use of the so-called Gspann parameter γ [24] when the finite heat bath theory (FHBT) is used to model experimental data for carbon clusters and fullerenes [16,25]. There are obvious energy–entropy tradeoffs and a method which circumvents the necessity of knowing the activation entropy $\Delta S^{\#}$, the Gspann parameter γ, or the pre-exponential A factor in the Arrhenius equation for reaction (3), is preferable for the determination of the activation (or binding) energy.

3.2. Appearance energies

Mass spectrometry has been instrumental in obtaining thermochemical data—bond energies and heats of formation—not only for ionic systems but also for neutrals. A wealth of information [26] is based on measurements of ionization energies (IEs) and AEs. For example, in the case of a simple bond cleavage reaction for a relatively small molecule M, giving an ionic fragment F^+ and a neutral fragment N, the ionic and neutral bond energies are, respectively, given by

$$D(F^+–N) = AE(F^+) - IE(M) \quad (5)$$

$$D(F–N) = AE(F^+) - IE(F) \quad (6)$$

Equations (5) and (6) cannot be applied to C_{60}, although erroneous attempts to do so have been carried out [27]. This point was elaborated upon before [28]. C_{60} demonstrates large conventional [29] and intrinsic [30] kinetic shifts. As a result, the appearance energy for C_{58}^+ cannot be calculated by adding the ionization energy of C_{60} to the activation energy for the C_2 loss reaction. Elaborate kinetic modeling of the experimental data is required to deduce the activation energy from the appearance energy.

The first measurement of an appearance energy was by vacuum ultraviolet (VUV) photoionization [31]. A single point at the 304 Å Ne II line, which corresponds to 40.8 eV, was measured and gave a C_{58}^+/C_{60}^+ ratio of 0.07 ± 0.04. No fragmentation was observed at 26.95 eV. The experimental temperature employed was 900 K. The results were modeled by two alternative transition states, either by removing a 1722 or a 263 cm^{-1} frequency from the reactant

frequencies and using $\sigma = 30$ as the reaction degeneracy. These models were employed in RRKM calculations and led to a minimum dissociation energy of 6.0–6.5 eV and a kinetic shift in the neighborhood of 30 eV [31]. Other groups employed these models in further studies and it was instructive to calculate the corresponding activation entropies, pre-exponential Arrhenius A factors, and Gspann γ parameters [18]. The activation entropies for the two photoionization models of [31] are $\Delta S^{\#} = -0.8$ and -3.1 e.u., respectively, i.e. these are relatively tight transition states. The Arrhenius equation gives for the canonical rate constant:

$$k(T_b) = A \exp(-\Delta E_{\text{vap}}/k_B T_b) \quad (7)$$

where T_b is an equivalent isokinetic bath temperature and k_B is Boltzmann's constant. The isokinetic bath temperature is defined in FHBT as the temperature to which a heat bath should be set so that the canonical rate constant, $k(T_b)$, is equal to the microcanonical rate constant, $k(E)$, sampled in the experiment. By using Eq. (7) with $T_b \approx 2600$ K; by using the relation

$$A = \sigma e(k_B T_b/h) \exp(\Delta S^{\#}/k_B) \quad (8)$$

where h is Planck's constant, and the definition of the Gspann parameter

$$\ln A - \ln k(T_b) = \gamma \quad (9)$$

with the number of equivalent ways of choosing the reaction coordinate being $\sigma = 30$ and $\Delta S^{\#} = -0.8$ or -3.1 eu yielded $\gamma = 23.5 \pm 0.5$ [18] and $A = 1.6 \times 10^{15}$ s^{-1}. These numbers should be contrasted with some of the most recent values [3]: $\Delta S^{\#} = 18.8$ e.u., $\gamma = 33$ and $A = 2.1 \times 10^{19}$ s^{-1}.

The appearance energy of C_{58}^+ from C_{60} has been remeasured over the years by using mainly electron impact ionization. Strong temperature effects on AEs from C_{60} have been predicted [18] and observed [32]. The results are consistently high–in excess of 40 eV for temperatures lower than ~1000 K. Selected values are: 43.7 ± 1.5 eV [33–35] at 890 K (average thermal energy 6.2 eV), and 47.2 eV [36] at 620 K (average thermal energy 3.2 eV). An exception is the AE determined by Baba et al. [27] which is considerably lower, because the ionizing electron currents employed were much too high and led to second order, i.e. consecutive ionization and excitation, processes [28]. The AEs are time dependent [33]. This has been demonstrated by ion trapping [36]; at a temperature of 620 K the AE decreases from 47.2 eV at zero trapping time to a lower limit of 45.1 eV which is already reached at 150 μs and stays independent of further time extension. The self-consistent determination of fullerene binding energies from appearance energies [37] will be discussed in greater detail as it involves modeling of breakdown curves. Suffice it to say that FHBT models with very different transition states for reaction (3), having Gspann parameters $\gamma =$ 25.6, 27.74, and 34.20 (i.e. pre-exponential A factors of ~1.3×10^{16}, 1.1×10^{17}, and 7.1×10^{19} s^{-1}) could fit the results nearly equally well, leading to C_2 binding energies of 7.06, 7.60, and 9.20 eV, respectively. Furthermore, a totally different modeling procedure of the thermal energy dependence of electron impact fragmentation [32] led to a binding energy of 4.0 eV together with a very low pre-exponential factor $A = 2.5 \times 10^{13}$ s^{-1}. What transpires is that different experiments give similar experimental results for the AEs, however the resultant C_2 binding energies are different since transition structures with different degrees of looseness were employed in the modeling.

3.3. Kinetic energy release distributions

Unimolecular reactions that possess no reverse activation energies, lead to KERDs which are Boltzmann-like and can be modeled by statistical theories such as phase space theory (PST) or by thermal kinetics in small systems, i.e. by the FHBT of Klots [25,38]. Bowers and co-workers [39] were the first to be modeled by the PST, the KERD obtained by tandem mass spectrometry for reaction (3), in order to deduce $D(C_{58}^+–C_2)$. The average kinetic energy release was determined to be $\langle\epsilon\rangle = 0.4 \pm 0.1$ eV. The average internal energy in the metastable parent ion was calculated to be 39 ± 2 eV and a binding energy of $D(C_{58}^+–C_2) = 4.6 \pm 0.5$ eV was obtained through the modeling of the KERD. Many experimental determinations of the KERD and of $\langle\epsilon\rangle$ followed. Al-

Table 1
Experimental results for the average KER of reaction (3), $\langle\epsilon\rangle$ eV and for the binding energy ΔE_{vap} { = $D(C_{58}^{+} - C_2)$}, eV deduced from KERDs

$\langle\epsilon\rangle$	$T^{\#}$(K)	γ	ΔE_{vap}	Source
0.4 ± 0.1	...	...	4.6 ± 0.5	Bowers, 1990 [39]
0.43 ± 0.05	...	23.5	4.6 ± 0.5	Lifshitz, 1991 [40]
0.395	2727	23.5	5.9	Klots, 1991 [41]
0.362	2390	23.5	5.23	Lifshitz, 1992 [15]
0.36	2797	23.5	6.07	Lifshitz, 1993 [25]
0.44 ± 0.01	3227	23.5 ± 1.5	7.1 ± 0.5	Lifshitz, 1995–1998 [42–44]
...	3300	23.5	7.2 ± 0.2	Lifshitz, 1999 [45]
...	3300	33	10.3	Lifshitz, 1999 [45]
0.40;0.41	2940	33	9.2	Märk, Lifshitz, 1999 [4,46]
0.40;0.41	2940	37.6	10.6	Märk, Lifshitz 1999 [4,46]

though some later determinations were carried out at somewhat better energy resolutions, the experimental results were basically the same, within experimental errors. On the other hand, the binding energy deduced from these results increased considerably with the year of measurement (see Table 1) because of the way these results were analyzed.

The analysis of the experimental KERDs may be performed by using two different approaches developed by Klots, namely, a model free approach [41,47] and a more generalized model, which treats the unimolecular decomposition in spherically symmetric potentials (SSPs) which are realistic and tractable [45,48]. We found that the more realistic the potential is, the closer is the binding energy deduced from it to the value deduced from the model free approach [45]. In the model free approach the KERD is written in the following form:

$$p(\epsilon) = \epsilon^{l} \exp(-\epsilon/k_B T^{\ddagger}) \qquad (0 < l < 1) \qquad (10)$$

where ϵ is the kinetic energy release, l is a parameter which ranges from zero to unity, and $T^{\ddagger}$ is the transition state temperature defined by the average kinetic energy on passing through the transition state. The values of l and $T^{\ddagger}$ are obtained by fitting the experimental KERD with Eq. (10). The value of l, which was found to give the best fit for all the KERDs, is $l \cong 0.5$. This corresponds to the expected value for the most statistical situation, since the translational density of states is proportional to $\epsilon^{0.5}$ [49]. The isokinetic bath temperature is given by [25,41]

$$T_b = T^{\ddagger} \frac{\exp(\gamma/C) - 1}{\gamma/C} \qquad (11)$$

where C is the heat capacity in units of k_B minus 1. Finally, combining Eqs. (7) and (9), one gets the so-called Trouton relation between the isokinetic bath temperature and the binding energy:

$$\Delta E_{vap} = \gamma k_B T_b \qquad (12)$$

A typical experimental KERD and the ones calculated by using the model free approach and the SSP model are shown in Fig. 2. There is good agreement between the experimental KERD and the models. Both models nearly overlap so that it is hard to distinguish between them [45].

Inspection of Table 1 demonstrates that the major change in recent modeling of the data lies in the value of γ employed. This has changed from 23.5—the recommended value for clusters [24]—to a value between 33 and 37.6, found to be appropriate for reaction (3), to be discussed in greater detail below. In other words, as in the case of the appearance energies

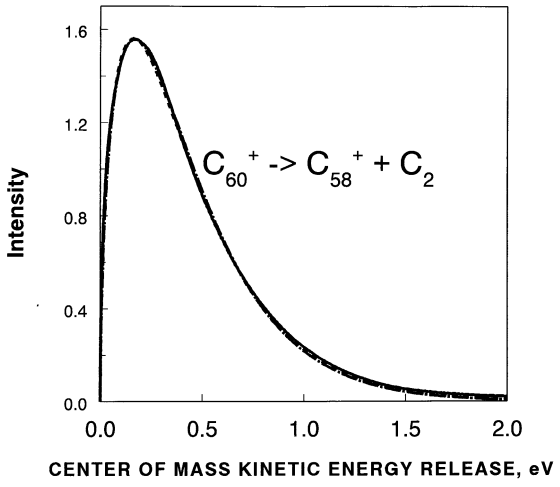

Fig. 2. Center-of-mass kinetic energy release distributions for the reaction $C_{60}^{+} \rightarrow C_{58}^{+} + C_2$; solid line: the experimental KERD, dashed line: the KERD obtained using the model free approach, dot-dash line: the KERD obtained from the SSP model (adapted from [45]).

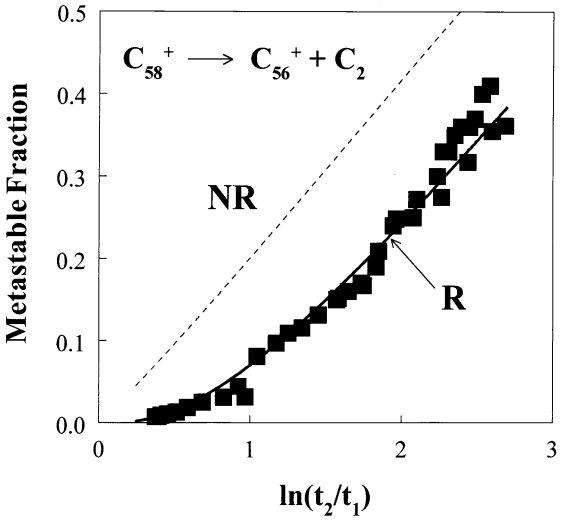

Fig. 3. Metastable decay probability of C_{58}^{+} as a function of $\ln(t_2/t_1)$. closed square: experimental results; solid line: model that takes into account radiative cooling; dotted line: model obtained without radiative decay. The activation parameters used in the modeling for reaction (3) are $\Delta E_{vap}(C_{60}^{+}) = 9.5$ eV and $\Delta S^{\#} = 18.8$ e.u.

discussed above, the KERDs do not give a unique answer for the binding energy if the degree of looseness expressed in the size of the Gspann parameter is equivocal.

3.4. Metastable fractions

The MF or metastable decay probability, is given by the ratio of daughter to total ions (daughter plus parent), i.e. $D/(D + P)$, of metastable ions dissociating in field free regions of a mass spectrometer. Metastable decompositions of fullerene cations were studied first by Bowers and co-workers [50] on a double-focusing sector instrument. The data were analyzed by Klots [41] and the relative binding energies of fullerenes were extracted. MFs were re-measured on sector [51] as well as on time-of-flight [52] instruments and the results were modeled by using RRKM/quasi-equilibrium theory (QET) [53]. Time-resolved MFs for times up to 20 μs were measured by Hansen and Campbell [21]. The rates of the metastable fragmentation were found to be much smaller than those predicted. This observation was explained, as noted in Sec. 3.1, by the existence of an alternative cooling mechanism namely photon emission [21].

The MF is given according to the FHBT and the evaporative ensemble model (EEM) due to Klots [25,38,54,55] by

$$D/(D + P) = (C/\gamma^2) \ln \{t_2/[t_1 + (t_2 - t_1) \exp(-\gamma^2/C)]\} \quad (13)$$

where t_1 and t_2 are the times corresponding to the beginning and end of a metastable time window, respectively. According to the EEM expression (13), the MF is nearly linearly dependent on $\ln(t_2/t_1)$. The EEM allows cooling only by evaporation but not by radiative decay. Time-resolved measurements of MFs were extended up to 100 μs by using an ion trap/reflectron mass spectrometer [56]. The plot of the MF due to C_2 elimination from C_{58}^{+} versus $\ln(t_2/t_1)$ was found to be nonlinear and to approach MF = 0 asymptotically as $\ln(t_2/t_1)$ approaches zero contrary to the predictions (Fig. 3). It was demonstrated [56] that these experimental results could only be modeled by taking radiative decay

$$C_{60}^{*\,+} \rightarrow C_{60}^{+} + h\nu \quad (3a)$$

in addition to dissociative C_2-evaporative decay, reaction (3) into account. The original description of the dissociative decay of C_{60}^+ and C_{58}^+ assumed the activation entropy to be the same and to have a value $\Delta S^{\#} = -0.2$ e.u., which corresponds to a rather tight transition state. This study was extended to include time-resolved MFs of C_{48}^+, C_{50}^+, C_{52}^+, C_{54}^+, C_{56}^+, and C_{58}^+ that were measured on an ion trap/reflectron and modeled by using both microcanonical dissociative and radiative decay rate constants [3]. These ions satisfy the evaporative-ensemble requirement, i.e. they are formed as a result of C_2 evaporation from the corresponding precursor ions. The width of the corresponding ensemble is directly related to the C_2 binding energy. In contrast, C_{60}^+ is formed by direct ionization from the fullerene sample without undergoing a prior evaporation. As a result, the energy distribution of C_{60}^+ ions is very wide due to the large kinetic shift. Consequently, the MF for C_{60}^+ is very low and its modeling requires the knowledge of the energy deposition function upon ionization, which is unknown. Since C_{58}^+ is formed from C_{60}^+ in the ion source, the ion source distribution of C_{58}^+ used in the modeling, as described in [56], depends on the C_2 binding energy assumed for C_{60}^+. Therefore, although the MF of C_{60}^+ itself has not been modeled, the kinetic parameters for the C_{60}^+ fragmentation were obtained from modeling of the metastable fraction of C_{58}^+. Time-resolved MFs of the ions C_{48}^+–C_{58}^+ were modeled in an internally consistent fashion. The modeling involved numerical integration of kinetic equations. The calculation of radiative rates followed Chupka and Klots [57] and was based on the fact that emission is related via detailed balance to absorption. The oscillator strengths for electronic transitions in C_{60} have been determined by a variety of methods. Those for C_{60}^+ were estimated from the ones for C_{60}. The microcanonical $k(E)$ dissociative decay rate constants were calculated by RRKM. Experimental and calculated metastable decay probabilities [3] are plotted as a function of $\ln(t_2/t_1)$ in Fig. 4. The agreement between experimental [3,21] and calculated results [3] is observed to be quite good. The concomitant fitting procedure for the evaporative ensemble including C_{48}^+, C_{50}^+, C_{52}^+, C_{54}^+, C_{56}^+, and C_{58}^+ required the use of highly loose transition states with an activation entropy as high as $\Delta S^{\#} = 19$ e.u. as well as a C_2 binding energy of 9.5 eV for C_{60}^+. Eq. (4) leads to a value in slight excess of 10 eV, for the binding energy of neutral C_{60}. The C_2 binding energies for $C_n^+(n = 48–58)$ were found to be lower than that of C_{60}^+ as expected and the results are summarized in Fig. 5. In conclusion, C_{60}^+ is observed to sit on the leading edge of a magic shell, as originally suggested by Klots [41], but the binding energies of the shell members are much higher than originally deduced. The experimental and computational study of time-resolved MFs for the members of the $C_n^+(n = 48–58)$ evaporative ensemble allowed this nearly unique determination of the activation parameters of reaction (3)—activation energy (i.e. binding energy) and activation entropy—to be achieved [3].

Is the determination of activation parameters for reaction (3) obtained from time-resolved MFs indeed unique? The radiative decay constants for the ionic species were estimated from the neutral ones [3] since information on their electronic spectroscopy is lacking. Efforts are in progress to develop models [58] that circumvent the necessity for detailed information on oscillator strengths. If these prove to be useful the present radiative decay curves could be checked and improved. Berkowitz has criticized our procedure in the following way [59]: “The narrative has been put into reverse. Instead of experiment and QET with an assumed transition state to infer a thermochemical dissociation energy, a predetermined dissociation energy has been used to infer a transition state.” As stated in our original article [3] a sincere effort was made not to pre-assume either the dissociation energy or the activation entropy, but by modeling as complete a set of experimental data as possible, to obtain a unique answer for both. This was achieved by fitting by the same model not only the time-resolved MFs discussed in this section but also the breakdown curves to be discussed in Sec. 3.5. The loose transition state found for reaction (3) will be discussed in greater detail in Sec. 3.6.

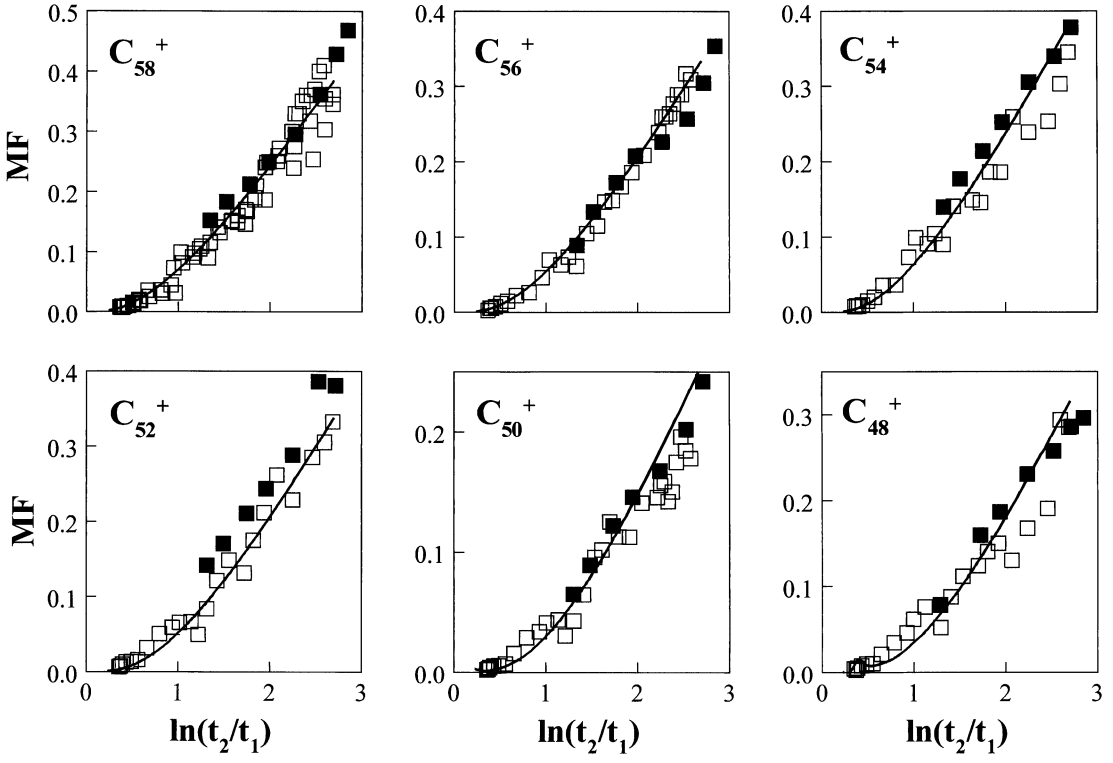

Fig. 4. Metastable decay probabilities as a function of $\ln(t_2/t_1)$. Open square: experimental results by Laskin and Lifshitz (published in part in [3]); filled square: experimental results by Hansen and Campbell (published in part in [21]); solid line: calculated.

3.5. Breakdown curves

The breakdown curve (BDC) of an ion gives its fractional abundance or probability of formation as a function of energy—either internal energy of the parent ion or energy transferred upon collision or ionization. Märk and co-workers determined breakdown curves for C_{60}^+, and fragment ions formed by consecutive C_2 eliminations from C_{60}^+, from second derivatives of electron impact ionization efficiency curves [33,37]. It has been demonstrated [37] that modeling the BDCs on their own can lead to different sets of $\Delta S^{\#}$ and ΔE_{vap}. FHBT models with very different transition states for reaction (3), having Gspann parameters $\gamma = 25.6$, 27.74, and 34.20, (i.e. pre-exponential A factors of $\sim 1.3 \times 10^{16}$, 1.1×10^{17}, and 7.1×10^{19} s^{-1}) could fit the results nearly equally well, leading to C_2 binding energies of 7.06, 7.60, and 9.20 eV, respectively. The original preferred set of $\Delta S^{\#} = -0.8$ e.u. and $\Delta E_{\text{vap}} = 7.06$ eV chosen to fit the BDCs [37], called TS-1, could not fit the MFs since TS-1 was much too tight. A much looser transition state, for reaction (3) and its analogues for the lower fullerene ions, had to be modeled for the MFs with $\Delta S^{\#}$ in the range of 14–19 e.u. A major conclusion from the fitting procedure of the MFs discussed before was that radiative decay is competing with dissociative decay even on a short time scale of microseconds. Radiative decay has not been included in the original calculations of the BDCs [33,37]; it was however included in their more recent modeling [3]. It turned out that MF modeling was very sensitive to the inclusion of the radiative decay contribution, while the BDCs were not as sensitive to radiative decay.

Fig. 6 represents the calculated and the experimental BDCs [3]. How reliable are the experimental breakdown curves that are obtained from second

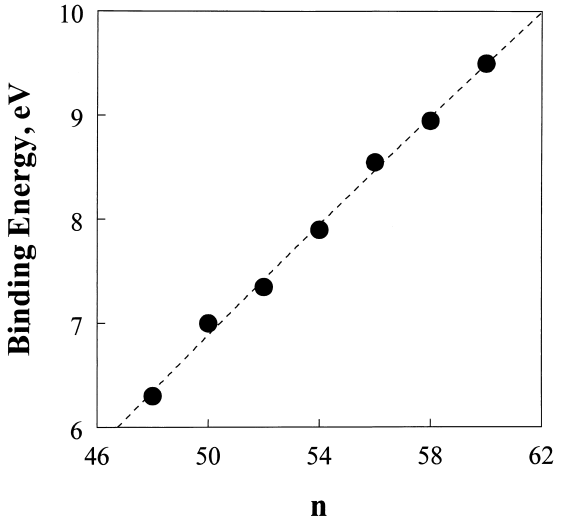

Fig. 5. C_2 binding energies in ionic fullerenes C_n^+ as a function of size n. The results are based solely on the analysis of time-resolved MFs. Those for C_{48}^+ and C_{50}^+ are lower than the ones quoted in Fig. 4 of [3] on the basis of BDCs and do not reproduce the expected "magic" character of $n = 50$.

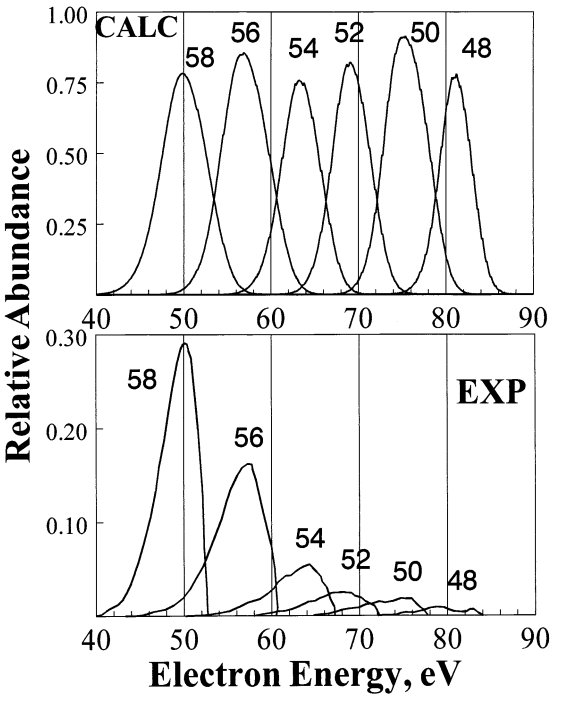

Fig. 6. Calculated (top) and experimental (bottom) breakdown curves for C_{58}^+, C_{56}^+, . . . , C_{48}^+ fragment ions of C_{60} (adapted from [3]).

derivatives of electron ionization efficiency curves? Due to nonideality of the ionization efficiency curves the second derivatives become negative at high energies. This leads to the abrupt zero-abundance high-energy cutoffs of the experimental BDCs (Fig. 6) which are absent in the calculated curves but should have no marked effect on the positions of the maxima of the experimental curves. The model is observed to reproduce the peak positions of the breakdown curves of the various ions. No effort was made to reproduce the lowering of the relative abundances of the experimental curves with decreasing size of the fullerene ion. This effect is known to be due to a declining energy deposition function [37]. Best agreement with both the MF data as well as the BDC data was obtained with a C_2 binding energy of 9.5 eV for C_{60}^+ and a $\Delta S^{\#} = 18.8$ e.u. For $\sigma = 30$ and $T_b = 1000$ K this activation entropy corresponds to a pre-exponential A factor of $A = 2.1 \times 10^{19}$ s^{-1} and if the most probable rate constant is $k_{mp} = 1 \times 10^5$ s^{-1}, then the corresponding Gspann parameter is $\gamma = 33$ [3].

A set of calculated rate/energy, $k(E)$ dependencies for the dissociative and radiative rate constants, for reactions (3) and (3a), respectively, [60], are presented in Fig. 7.

3.6. Choice of transition states (a theoretical interlude)

This section is devoted to the question of choice of transition states. What transpires from the discussion so far is that with the increasing values deduced over the years for ΔE_{vap} by the various experimental methods, there has been a concomitant increase in the degree of looseness of the transition state of reaction (3). In some of the experimental studies there has been a genuine effort to determine the activation parameters—activation energy and activation entropy—uniquely. Yet there has been a definite energy–entropy tradeoff. The activation entropy has gone up over the years as have the Gspann parameter γ and the Arrhenius pre-exponential A factor for the C_2 elimination from C_{60}^+. There is also the criticism viewed by Berkowitz [59] quoted in Sec. 3.4, that a predetermined dissociation energy has been used to infer a

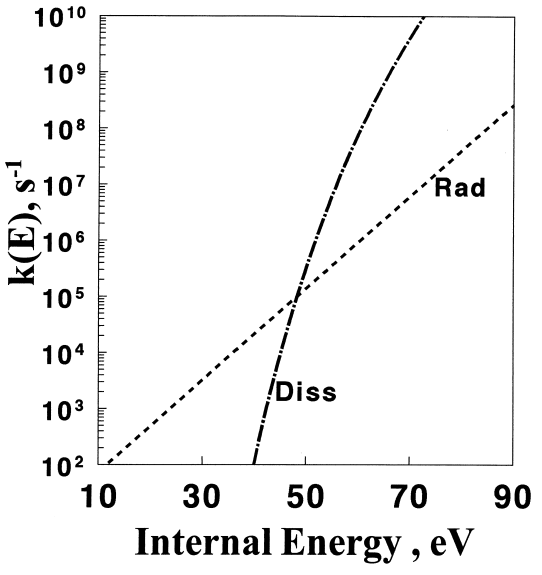

Fig. 7. Microcanonical rate constant, $k(E)$, in s^{-1}, as a function of energy, E, in eV, for dissociative decay (dot-dashed line) and radiative decay (dashed line) of C_{60}^+. Dissociation involves elimination of C_2, reaction (3). The activation parameters employed in this calculation for reaction (3) are: $A = 5 \times 10^{19}$ s^{-1} (at k_BT_b = 0.2 eV) and $\Delta E_{vap} = 10.3$ eV [61]. The A factor corresponds with $\Delta S^{\#} = 18.8$ e.u. and $\sigma = 30$. The evaporation energy is the value obtained from analysis of the KERDs with $\gamma = 33$ ([45] and Table 1). The radiative decay rate can be cast in the form: $\log k(E) = 0.082E + 1.045$.

transition state. It makes sense therefore to explore the validity of this transition state.

Can the looseness of the transition state be probed without involvement of the activation energy? This has been attempted through the measurement of the time dependence of the C_{60}^+ parent ion signal, $P(t) = 1 - MF$, in two field free regions of a double focusing instrument and the use of Eq. (13) to derive γ [4,60]. The value of γ is time dependent [60,61] as is obvious from its definition by Eq. (9) and it is therefore instrument dependent. $\gamma = 37.6$ was obtained for the CH5 mass spectrometer as an average over six data sets, with a root mean square standard deviation of 2.5 (see footnote 6 of [4]). Radiative decay has not been taken into account so that $\gamma = 37.6$ is an upper limit. If the most probable rate constant is $k_{mp}(T_b) = 1 \times 10^5$ s^{-1}, Eq. (9) gives for the Arrhenius prefactor the value $A = 2 \times 10^{21}$ s^{-1}. This corresponds to an extremely loose transition state and needs to be explored further. A literature search has not disclosed any unimolecular reaction previously known to have such a high pre-exponential A factor (see e.g. [62]). On the other hand, none of the molecules previously studied is as unique as C_{60}.

The dissociation mechanism of C_{60} has been studied through ab initio quantum-chemical calculations [63–65]. C_2 elimination is a multiple step process. The last step involves formation of a C_{58} isomer containing a seven-membered ring (7-m.r.) to which a C_2 "stick" is loosely bound. The C_2 molecule that leaves the fullerene surface is due to a bond shared by a hexagon and a pentagon (5–6 bond). These findings can form the basis for a computation of the A factor by statistical thermodynamics ([38], p. 204; [62], p. 152; [66], p. 115). A useful equation has been given by Klots [67] for which we are using a minor variation,

$$A = \sigma(k_BT_b/h)[Q^f_{vib}Q_{rot}Q_{surf}/Q^i_{vib}] \times [(I_1 + I_2)/(\mu b^2 + I_1 + I_2] \quad (14)$$

where: σ is the reaction path degeneracy as before, Q^f_{vib} is the final vibrational partition function of the C_{58}/C_2 pair, Q_{rot} is the rotational partition function of C_2, Q_{surf} is the C_{58}/C_2 stick two-dimensional surface partition function, Q^i_{vib} is the initial vibrational partition function of C_{60}, I_1 and I_2 are the moments of inertia of C_{58} and C_2, respectively, whereas μb^2 is the moment of inertia of the C_{58}/C_2 pair, where μ is the reduced mass and $b = 3.8$ Å is the impact parameter.

The Arrhenius A factor is temperature dependent and calculations have been carried out for a temperature such that $k_BT_b = 0.2$ eV. The reaction path degeneracy is $\sigma = 60$ because there are 12 pentagons in C_{60} with five edges each (this contradicts the use until recently of $\sigma = 30$). The next factor in Eq. (14) is $k_BT_b/h = 4.8359 \times 10^{13}$ s^{-1}. For $C_{60} \rightarrow C_{58} + C_2$ five vibrational frequencies of ~1000 cm^{-1} are lost each with $Q_{vib} = 1/\{1 - \exp(-h\nu/k_BT_b)\} = 2.1645$. This leads to $Q^f_{vib}/Q^I_{vib} = (1/2.1645)^5 = 1/47.5$. C_2 is a two-dimensional rotor with a moment of inertia $I_2 = 1.53 \times 10^{-39}$ g cm^2 and rotational partition function $Q_{rot} = (8\pi^2k_BT_b/\sigma_{C2}h^2)I_2 =$

441; this rotational partition function has been calculated before [68]. The surface rotational partition function is $Q_{\text{surf}} = (8\pi^2 k_B T_b/h^2)\mu b^2 = 32081$. The final term in brackets on the right-hand side of Eq. (14) is a small correction term equaling 0.934. As a result, $A = 60 \times 4.8359 \times 10^{13} \times 441 \times 32081 \times (1/47.5) \times 0.934 = 8 \times 10^{20}\ \text{s}^{-1}$. The value $A = 8 \times 10^{20}\ \text{s}^{-1}$ is considered to be an upper limit. It is somewhat lower than the value $2.1 \times 10^{21}\ \text{s}^{-1}$ calculated above for $\gamma = 37.6$. The activation entropy deduced from time resolved MFs [3] $\Delta S^{\#} = 18.8$ e.u., combined with $\sigma = 60$ and $k_B T_b = 0.2$ eV, gives $A = 1.0 \times 10^{20}\ \text{s}^{-1}$. It is thus entirely plausible for reaction (3) to have an activation entropy of ~19 e.u., a Gspann parameter $\gamma = 33$–37.6 for the time range of several microseconds and an Arrhenius pre-exponential A factor at $k_B T_b = 0.2$ eV, in the range $10^{20} \leq A \leq 10^{21}\ \text{s}^{-1}$.

3.7. Competition between dissociation and thermionic emission

Thermionic emission occurs in those materials (e.g. tungsten) in which the heat of evaporation is higher than the work function. This holds also for clusters and fullerenes such as C_{60} in the neutral state, for which the ionization energy is lower than the C_2 binding energy. Thermionic emission manifests itself through delayed electron emission from excited gas-phase C_{60}. Dissociation and ionization of C_{60},

$$C_{60} \rightarrow C_{58} + C_2 \quad (1)$$

$$\rightarrow C_{60}^{+} + e^{-} \quad (1a)$$

respectively, are two competitive processes. Radiative decay,

$$\rightarrow C_{60} + h\nu \quad (1b)$$

is also possible for internally hot neutral C_{60}. The efficiency of thermionic emission has been determined experimentally [69] to reach 2.6 ± 1.1%.

The rate of delayed (thermionic) ionization of photoexcited C_{60} molecules was analyzed [2]. Delayed electron emission from hot C_{60} follows a power law in time t,

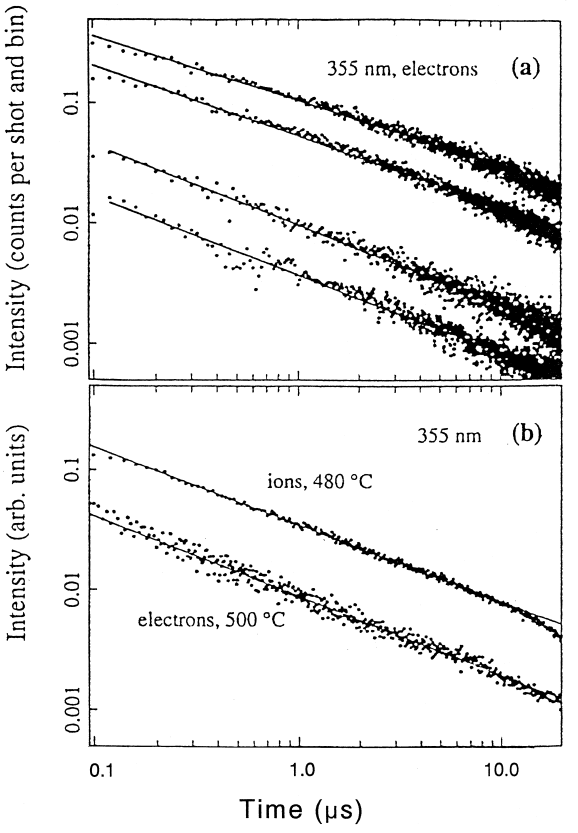

Fig. 8. Delayed electron and delayed ion spectra from C_{60} recorded following excitation by a frequency-tripled Nd:YAG laser at 355 nm over a range of source temperatures and laser fluences (adapted from [2]).

$$dI/dt \sim t^{-p} \quad (15)$$

indicating the presence of a continuum of rate constants. This dependence is very reminiscent of results used in early determinations of rate energy dependencies for ionic dissociations [70]. The exponent determined experimentally for thermionic emission, from a plot of log dI/dt versus log t (see Fig. 8), is $p = 0.64 \pm 0.10$. Theoretical analysis [2] shows that the exponent p is, approximately, equal to the ratio of the ionization energy, $\text{IE}(C_{60}) = 7.6 \pm 0.1$ eV [71] and the activation energy for C_2 emission, ΔE_{vap},

$$p = \text{IE}/\Delta E_{\text{vap}} \quad (16)$$

The C_2 binding energy in neutral C_{60} was deduced from this analysis to be $\Delta E_{\text{vap}} = 11.9 \pm 1.9$ eV. The

analysis did not necessitate any assumption concerning the degree of looseness of the transition state. It did assume however that radiative decay, reaction (1b), can be neglected. The energy deposition function in the laser excitation of C_{60} has been assumed to be flat [2], an assumption that has been criticized [72]. This criticism has been addressed [68]. A more recent analysis by Klots [73] yields for the exponent of Eq. (15),

$$p = (\mathrm{IE}/\Delta E_{\mathrm{vap}}) + 2/\gamma \quad (17)$$

This leads to an even higher value than 11.9 eV for ΔE_{vap}.

We found it very difficult to reproduce a thermionic emission yield of 2.6% [69] by using a critical energy of vaporization of 11.9 eV or higher, particularly since the time scale for thermionic emission [2] is microseconds and the $k(E)$ curves for reactions (1) and (1a) cross at much too high an energy and too high a rate constant if $\Delta E_{\mathrm{vap}} \geq 11.9$ eV. However, by using $\Delta E_{\mathrm{vap}} = 10$ eV, which is within the error limits of the value deduced by Hansen and Echt [2], from the analysis of Eq. (15), it is possible to reproduce the thermionic emission yield. The rate energy dependencies calculated for reactions Eqs. (1), (1a), and (1b) are reproduced in Fig. 9. The values employed for the pre-exponential A factors and activation energies are: $A(1) = 8 \times 10^{20}\ \mathrm{s}^{-1}$, $\Delta E_{\mathrm{vap}}(1) = 10$ eV; $A(1a) = 2 \times 10^{16}\ \mathrm{s}^{-1}$, $\mathrm{IE}(C_{60}) = 7.6$ eV. The curves are seen to cross at a very low rate constant. At the same energy for which the dissociative rate constant is $k(1) \cong 3.8 \times 10^{6}\ \mathrm{s}^{-1}$, the rate constant for thermionic emission is $k(1a) \cong 1 \times 10^{5}\ \mathrm{s}^{-1}$ leading to a thermionic emission yield of about 2.6%, in the range of $\sim 10\ \mu$s, as required. Does radiative decay compete in the case of neutral C_{60} with dissociation and thermionic emission? With the current choice of the pre-exponential A factor for reaction (1) and the current level of theory for the rate of radiative decay, the latter is not an important factor on the microsecond level for which the quantum yield of thermionic emission has been determined (see Fig. 9). Furthermore, radiative decay cannot be responsible for the negative slope p of $\log(dI/dt)$ versus $\log t$ being less than 1 because the activation energy for reaction (1b) is considerably lower than that of reaction (1a) and the slope should be nearly equal to the ratios of the activation energies of the two competing processes. Only reaction (1) whose activation energy is higher than that of reaction (1a) can be responsible for $p < 1$.

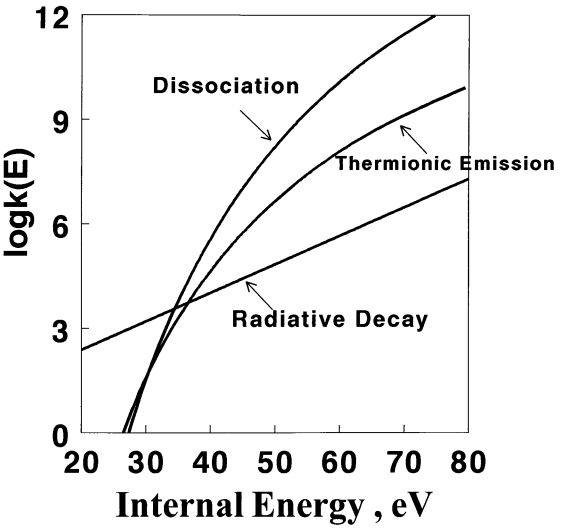

Fig. 9. Microcanonical rate constant, $k(E)$ in s^{-1}, as a function of energy, E in eV, for dissociative decay, thermionic emission and radiative decay of neutral C_{60}, reactions (1), (1a), and (1b), respectively. The activation parameters employed for dissociation and thermionic emission are: $A(1) = 8 \times 10^{20}\ \mathrm{s}^{-1}$, $\Delta E_{\mathrm{vap}}(1) = 10$ eV; $A(1a) = 2 \times 10^{16}\ \mathrm{s}^{-1}$, $\mathrm{IE}(C_{60}) = 7.6$ eV. The radiative decay rate can be cast in the form: $\log k(E) = 0.082E + 0.744$.

4. Conclusion

We have reviewed in this article the current status concerning the C_2 binding energy in C_{60} as derived from measurements on ionic systems. The measurements include KERDs [4], metastable fractions (MFs) [3], breakdown curves [3] and thermionic emission rates [2]. The recent experiments agree with a value $\Delta E_{\mathrm{vap}} \geq 10$ eV for neutral C_{60} and $\Delta E_{\mathrm{vap}} \geq 9.5$ eV for C_{60}^{+}. This result is in agreement with high level ab initio calculations [5]. The majority of experimental methods employed give results for ΔE_{vap} which depend on the degree of looseness chosen for the

transition state of reaction (3), as expressed by its activation entropy, its γ Gspann parameter and/or its pre-exponential A factor. Some genuine efforts were made to determine the activation parameters—activation entropy and activation energy—uniquely [3] and/or independently [4,60]. This has been particularly successful with measurements of time-resolved metastable fractions. The experimental determinations made of $\Delta S^{\#}$ and of γ have indicated a highly loose transition state. A statistical-thermodynamical calculation of the pre-exponential A factor that assumes a C_2 stick loosely bound to C_{58} reproduces the experimental results and gives $A \leq 8 \times 10^{20}$ s^{-1}. The picture of a C_2 stick loosely bound to C_{58} as a last intermediate in a multiple-step mechanism for reaction (1) is in agreement with ab initio calculations [63–65]. The analysis of the time dependence of thermionic emission rates yields a value for ΔE_{vap} that is independent of any assumptions concerning the transition state. However, the error limits are rather large: $\Delta E_{vap} = 11.9 \pm 1.9$ eV [2]. A value of $\Delta E_{vap} = 10$ eV for neutral C_{60} is in the range of these error limits and in agreement with the results from time-resolved MFs [3] as well as ab initio calculations [5]. When combined with the pre-exponential factor $A = 8 \times 10^{20}$ s^{-1} it can reproduce the experimentally observed efficiency of thermionic emission [69]. However a higher value for ΔE_{vap} and a lower value for the A factor, which are more in line with some of the experimental results, when combined with the same activation parameters for thermionic emission, do not reproduce the thermionic efficiency.

Acknowledgements

The research has been supported by the James Franck Foundation and by The Austrian Friends of The Hebrew University. The Farkas Center is supported by the Minerva Gesellschaft für die Forschung GmbH, München. The authors would like to thank Dr. Julia Laskin, Professor C. E. Klots, Professor E. E. B. Campbell, and Professor T. D. Märk for very helpful discussions.

References

[1] Nomenclature: The terms “binding energy” and “dissociation energy” are equivalent. The first is usually used for clusters whereas the second is for stable molecules. Because C_{60} can be considered to be either a carbon cluster or a stable molecule, both terms apply. In addition, the term “evaporation energy,” ΔE_{vap} is also being used because clusters are considered to bridge the gap between isolated molecules in the gas phase and condensed phases. Finally, the activation energy, E_a, of reaction (1) is also considered to be equal to the C_2 binding energy since there is no activation energy for the reverse reaction.
[2] K. Hansen, O. Echt, Phys. Rev. Lett. 78 (1997) 2337.
[3] J. Laskin, B. Hadas, T.D. Märk, C. Lifshitz, Int. J. Mass Spectrom. 177 (1998) L9.
[4] S. Matt, O. Echt, M. Sonderegger, R. David, P. Scheier, J. Laskin, C. Lifshitz, T.D. Märk, Chem. Phys. Lett. 303 (1999) 379.
[5] A.D. Boese, G.E. Scuseria, Chem. Phys. Lett. 294 (1998) 233.
[6] R.L. Whetten, C. Yeretzian, Clusters and Fullerenes, World Scientific, Singapore, 1993.
[7] F.H. Hennrich, H.-J. Eisler, S. Gilb, P. Gerhardt, R. Wellmann, R. Schulz, M.M. Kappes, Ber. Bunsenges. Phys. Chem. 101 (1997) 1605.
[8] T. Sommer, T. Kruse, P. Roth, J. Phys. Chem. 99 (1995) 13509.
[9] E. Kolodney, B. Tsipinyuk, A. Budrevich, J. Chem. Phys. 100 (1994) 8542.
[10] R.E. Stanton, J. Chem. Phys. 96 (1992) 111.
[11] J.Y. Yi, J. Bernholc, J. Chem. Phys. 96 (1992) 8634.
[12] W.C. Eckhoff, G.E. Scuseria, Chem. Phys. Lett. 216 (1993) 399.
[13] C.H. Xu, G.E. Scuseria, Phys. Rev. Lett. 72 (1994) 669.
[14] B.L. Zhang, C.H. Xu, C.Z. Wang, C.T. Chan, K.M. Ho, Phys. Rev. B 46 (1992) 7333.
[15] P. Sandler, C. Lifshitz, C.E. Klots, Chem. Phys. Lett. 200 (1992) 445.
[16] C. Lifshitz, Mass Spectrom. Rev. 12 (1993) 261.
[17] R.D. Beck, P. St. John, M.M. Alvarez, F. Diederich, R.L. Whetten, J. Phys. Chem. 95 (1991) 8402.
[18] C. Lifshitz, I. Gotkis, P. Sandler, J. Laskin, Chem. Phys. Lett. 200 (1992) 406.
[19] R. Mitzner, E.E.B. Campbell, J. Chem. Phys. 103 (1995) 2445.
[20] E. Kolodney, A. Budrevich, B. Tsipinyuk, Phys. Rev. Lett. 74 (1995) 510.
[21] K. Hansen, E.E.B. Campbell, J. Chem. Phys. 104 (1996) 5012.
[22] T. Baer, Adv. Chem. Phys. 64 (1986) 111; P.M. Mayer, T. Baer, Chem. Phys. Lett. 261 (1996) 155; O.A. Mazyar, T. Baer, J. Am. Soc. Mass Spectrom. 10 (1999) 200.
[23] T. Drewello, W. Krätschmer, M. Fieber-Erdmann, A. Ding, Int. J. Mass Spectrom. Ion Processes 124 (1993) R1.
[24] C.E. Klots, Int. J. Mass Spectrom. Ion Processes 100 (1990) 457.
[25] C. Lifshitz, in Current Topics in Ion Chemistry and Physics:

Clusters, T. Baer, C.Y. Ng, I. Powis (Eds.), Wiley, New York, 1993.
[26] S.G. Lias, J.E. Bartmess, J.F. Liebman, J.L. Holmes, R.D. Levin, W.G. Mallard, J. Phys. Chem. Ref. Data 17 (1988) (Suppl. 1).
[27] M.S. Baba, T.S.L. Narashima, R. Balasubramanian, C.K. Mathews, J. Phys. Chem. 99 (1995) 3020.
[28] S. Matt, D. Muigg, A. Ding, C. Lifshitz, P. Scheier, T.D. Märk, J. Phys. Chem. 100 (1996) 8692.
[29] W.A. Chupka, J. Chem. Phys. 30 (1959) 191.
[30] F.S. Huang, R.C. Dunbar, J. Am. Chem. Soc. 112 (1990) 8167.
[31] R.K. Yoo, B. Ruscic, J. Berkowitz, J. Chem. Phys. 96 (1992) 911.
[32] E. Kolodney, B. Tsipinyuk, A. Budrevich, J. Chem. Phys. 102 (1995) 9263.
[33] M. Foltin, M. Lezius, P. Scheier, T.D. Märk, J. Chem. Phys. 98 (1993) 9624.
[34] P. Scheier, B.Dünser, R. Wörgötter, M. Lezius, R. Robl, T.D. Märk, Int. J. Mass Spectrom. Ion Processes 138 (1994) 77.
[35] R. Wörgötter, B. Dünser, P. Scheier, T.D. Märk, J. Chem. Phys. 101 (1994) 8674.
[36] J. Laskin, J.M. Behm, K.R. Lykke, C. Lifshitz, Chem. Phys. Lett. 252 (1996) 277.
[37] R. Wörgötter, B. Dünser, P. Scheier, T.D. Märk, M. Foltin, C.E. Klots, J. Laskin, C. Lifshitz, J. Chem. Phys. 104 (1996) 1225.
[38] T. Baer, W.L. Hase, Unimolecular Reaction Dynamics, Oxford University Press, New York, 1996.
[39] P.P. Radi, M.-T. Hsu, M.E. Rincon, P.R. Kemper, M.T. Bowers, Chem. Phys. Lett. 174 (1990) 223.
[40] C. Lifshitz, M. Iraqi, T. Peres, J.E. Fischer, Int. J. Mass Spectrom. Ion Processes 107 (1991) 565.
[41] C.E. Klots, Z. Phys. D 21 (1991) 335.
[42] J. Laskin, H.A. Jiménez-Vázquez, R. Shimshi, M. Saunders, M.S. de Vries, C. Lifshitz, Chem. Phys. Lett. 242 (1995) 249.
[43] J. Laskin, C. Weickhardt, C. Lifshitz, Int. J. Mass Spectrom. Ion Processes 161 (1997) L7.
[44] C. Lifshitz, Fullerene Sci. Technol. 6 (1998) 137.
[45] J. Laskin, T. Peres, A. Khong, H.A. Jiménez-Vázquez, R.J. Cross, M. Saunders, D.S. Bethune, M.S. de Vries, C. Lifshitz, Int. J. Mass Spectrom. Ion Processes 185/186/187 (1999) 61.
[46] S. Matt, M. Sonderegger, R. David, O. Echt, P. Scheier, J. Laskin, C. Lifshitz, T.D. Märk, Int. J. Mass Spectrom Ion Processes 185/186/187 (1999) 813.
[47] P. Sandler, T. Peres, G. Weissman, C. Lifshitz, Ber. Bunsenges. Phys. Chem. 96 (1992) 1195.
[48] C.E. Klots, J. Chem. Phys. 98 (1993) 1110; 100 (1994) 1035.
[49] (a) R.D. Levine, R.B. Bernstein, Molecular Reaction Dynamics and Chemical Reactivity, Oxford University Press, New York, 1987, pp. 274, 275; (b) T. Baer, W.L. Hase, Unimolecular Reaction Dynamics, Oxford University Press, New York, 1996, pp. 173, 174; (c) P. Urbain, F. Remacle, B. Leyh, J.C. Lorquet, J. Phys. Chem. 100 (1996) 8003.
[50] P.P. Radi, M.E. Rincon, M.-T. Hsu, J. Brodbelt-Lustig, P.R. Kemper, M.T. Bowers, J. Chem. Phys. 92 (1990) 4817.
[51] C. Lifshitz, J. Laskin, T. Peres, Org. Mass Spectrom 28 (1993) 1001.
[52] E.E.B. Campbell, G. Ulmer, H.-G. Busman, J.V. Hertel, Chem. Phys. Lett. 175 (1990) 505.
[53] J. Laskin, C. Lifshitz, Int. J. Mass Spectrom. Ion Processes 138 (1994) 95.
[54] C.E. Klots, Z. Phys. D 5 (1987) 83.
[55] C.E. Klots, J. Phys. Chem. 92 (1988) 5864.
[56] J. Laskin, C. Lifshitz, Chem. Phys. Lett. 277 (1997) 564.
[57] W.A. Chupka, C.E. Klots, Int. J. Mass Spectrom. Ion Processes 167/168 (1997) 595.
[58] J.U. Andersen, E. Bonderup, Eur. Phys. J. D., submitted.
[59] J. Berkowitz, J. Chem. Phys. 111 (1999) 1446.
[60] V. Foltin, M. Foltin, S. Matt, P. Scheier, K. Becker, H. Deutsch, T.D. Märk, Chem. Phys. Lett. 289 (1998) 181.
[61] S. Matt, R. Parajuli, A Stamatovic, P. Scheier, T.D. Märk, J. Laskin, C. Lifshitz, Eur. Mass Spectrom., in press.
[62] P.J. Robinson, K.A. Holbrook, Unimolecular Reactions, Wiley-Interscience, London, 1972.
[63] R.L. Murry, D.L. Strout, G.K. Odom, G.E. Scuseria, Nature (London) 366 (1993) 665.
[64] W.C. Eckhoff, G.E. Scuseria, Chem. Phys. Lett. 216 (1993) 399.
[65] C. Xu, G.E. Scuseria, Phys. Rev. Lett. 72 (1994) 669.
[66] K.A. Holbrook, M.J. Pilling, S.H. Robertson, Unimolecular Reactions, 2nd ed., Wiley, Chichester, 1996.
[67] C.E. Klots, Z. Phys. D 20 (1991) 105.
[68] K. Hansen, O. Echt, Phys. Rev. Lett. 82 (1999) 460.
[69] R. Deng, O. Echt, J. Phys. Chem. 102 (1998) 2533.
[70] I. Hertel, Ch. Ottinger, Z. Naturforsch. 22a (1967) 1141.
[71] J. de Vries, H. Steger, B. Kamke, C. Menzel, B. Weisser, W. Kamke, I.V. Hertel, Chem. Phys. Lett. 188 (1992) 159.
[72] P. Stampfli, T.D. Märk, Phys. Rev. Lett. 82 (1999) 459.
[73] C.E. Klots, personal communication, July 1999.